Class IIa HDACs repressive activities on MEF2-depedent transcription are associated with poor prognosis of ER$^+$ breast tumors

Andrea Clocchiatti,[*,†] Eros Di Giorgio,[*,†] Sabrina Ingrao,[‡] Franz-Josef Meyer-Almes,[§] Claudio Tripodo,[‡] and Claudio Brancolini[*,†,1]

*Dipartimento di Scienze Mediche e Biologiche and †Microgravity, Aging, Training, and Immobility (MATI) Center of Excellence Università degli Studi di Udine, Udine, Italy; ‡Tumor Immunology Section, Department of Human Pathology, University of Palermo School of Medicine, Palermo, Italy; and §Department of Chemical Engineering and Biotechnology, University of Applied Sciences, Darmstadt, Germany

ABSTRACT **MEF2s transcription factors and class IIa HDACs compose a fundamental axis for several differentiation pathways. Functional relationships between this axis and cancer are largely unexplored. We have found that class IIa HDACs are heterogeneously expressed and display redundant activities in breast cancer cells. Applying gene set enrichment analysis to compare the expression profile of a list of putative MEF2 target genes, we have discovered a correlation between the down-regulation of the MEF2 signature and the aggressiveness of ER$^+$ breast tumors. Kaplan-Meier analysis in ER$^+$ breast tumors evidenced an association between increased class IIa HDACs expression and reduced survival. The important role of the MEF2-HDAC axis in ER$^+$ breast cancer was confirmed in cultured cells. MCF7 ER$^+$ cells were susceptible to silencing of class IIa HDACs in terms of both MEF2-dependent transcription and apoptosis. Conversely, in ER$^-$ MDA-MB-231 cells, the repressive influence of class IIa HDACs was dispensable. Similarly, a class IIa HDAC-specific inhibitor preferentially promoted the up-regulation of several MEF2 target genes and apoptosis in ER$^+$ cell lines. The prosurvival function of class IIa HDACs could be explained by the repression of NR4A1/Nur77, a proapoptotic MEF2 target. In summary, our studies underscore a contribution of class IIa HDACs to aggressiveness of ER$^+$ tumors.—Clocchiatti, A., Di Giorgio, E., Ingrao, S., Meyer-Almes, F.-J., Tripodo, C., Brancolini, C. Class IIa HDACs repressive activities on MEF2-depedent transcription are associated with poor prognosis of ER$^+$ breast tumors. *FASEB J.* 27, 942–954 (2013). www.fasebj.org**

Key Words: KLF2 · proliferation · Nur77 · apoptosis · GSEA

Class IIa histone deacetylases (HDACs; HDAC4, HDAC5, HDAC7, and HDAC9) are characterized by homology with the yeast enzyme Hda1, tissue-specific expression/functions, and nuclear-cytoplasmic shuttling (1). Cytoplasmic localization of class IIa is coupled to transcriptional activation, while nuclear accumulation promotes transcriptional repression (2). Nuclear-cytoplasmic shuttling is monitored by various kinases that can phosphorylate class IIa HDACs at 14-3-3 binding sites (3, 4). Other post-translational modifications, such as: sumoylation, selective proteolysis, and poly-ubiquitination, keep class IIa HDACs activities in check (5, 6). In addition, their expression is also subjected to transcriptional and translational control (7, 8). Various transcription factors have been reported to interact with class IIa HDACs. The most important are members of the myocyte enhancer factor 2 (MEF2) family (9). Several studies have certified the key role played by the MEF2-HDAC axis during differentiation (10, 11). By contrast, tumor-associated alterations of the axis have been observed only recently (12–14).

Breast cancer comprises a heterogeneous group of diseases characterized by distinct molecular aberrations (15). Sequencing of protein-coding genes has revealed statistically significant mutations of HDAC4 in breast cancer (16). Other studies have reported altered expression of MEF2 members and of HDAC4 (17, 18). Despite some available clues, the contribution of the MEF2-HDAC axis to breast cancer is largely unexplored. In this study, we have investigated the status of the axis in breast cancer cell lines and tumors. Overall, our data imply that targeting class IIa HDACs could represent an interesting therapeutic strategy for impairing proliferation of estrogen receptor-positive (ER$^+$) aggressive tumors.

Abbreviations: AMPK, AMP-activated protein kinase; BrdU, bromodeoxyuridine; ER, estrogen receptor; GSEA, gene set enrichment analysis; HDAC, histone deacetylase; HDI, histone deacetylase inhibitor; KLF2, Krüppel-like factor 2; MEF2, myocyte enhancer factor 2

[1] Correspondence: Dipartimento di Scienze Mediche e Biologiche Universita' di Udine. P.le Kolbe 4–33100, Udine, Italy. E-mail: claudio.brancolini@uniud.it

doi: 10.1096/fj.12-209346

This article includes supplemental data. Please visit *http://www.fasebj.org* to obtain this information.

0892-6638/13/0027-0942 © FASEB

MATERIALS AND METHODS

Cell culture, infections, and siRNA transfection

MCF-10A cells were grown as described previously (6). Breast cancer cell lines were maintained in Dulbecco's modified Eagle's medium (DMEM) supplemented with 10% FBS plus penicillin/streptomycin and L-glutamine, with the exception of ZR-75-1 and HCC1937 cells, which were grown in RPMI 1640. The CRM1 inhibitor, leptomycin-B (LC Laboratories, Woburn, MA, USA), was used at 5 ng/ml. AICAR (Sigma-Aldrich, St. Louis, MO, USA) was used. IC_{50} values were obtained using the Rezazurin test. MCF7 and MDA-MB-231 cells expressing GFP or HDAC4-GFP transgenes were generated by retroviral infection as described previously (6). Cells were transfected 24 h after plating by adding the OptiMem medium containing Lipofectamine plus the stealth RNAi oligos (Invitrogen, Carlsbad, CA, USA). Cells were collected after 48 h from transfection.

Immunohistochemistry

Sections of breast tissue, 4 μm thick, were deparaffinized and rehydrated. Subsequently, the slides were microwave-treated in citrate buffer (pH 6; DakoCytomation, Glostrup, Denmark). After neutralization of the endogenous peroxidase, sections were first incubated with protein block Novocastra (UK) for 10 min and next with the anti-human HDAC4 (dilution 1:100). Incubation time was overnight at 4°C. Normal mouse serum was used as negative control. Staining was performed by streptavidin-Hrp/biotyn detection system (LSAB+ System-Hrp; Dako). After counterstaining with hematoxylin (Novocastra, Newcastle upon Tyne, UK), sections were viewed under a Leica DM3000 optical microscope (Leica Microsystems, Wetzlar, Germany), and captions were collected using a Leica DFC320 digital camera (Leica).

Immunoblotting, immunoprecipitation, and immunofluorescence

Immunoblotting was performed as described previously (6). Antibodies used in this work were anti: HDAC3, HDAC5 and HDAC7 (Cell Signaling Technology, Danvers, MA, USA), HDAC9 (Abcam, Cambridge, UK), MEF2A (Santa Cruz Biotechnology, Santa Cruz, CA, USA), MEF2C (Cell Signaling Technology), MEF2D and Ran (BD Biosciences, San Jose, CA, USA), EFGR (Santa Cruz Biotechnology), and Bcl-2 (Sigma-Aldrich). For immunoprecipitations, cells were collected directly from culture dishes with a rubber scraper into low-salt lysis buffer (20 mM TrisHCl, pH 7.5; 2 mM EDTA; 10 mM $MgCl_2$; 10 mM KCl; and 1% Triton-X100) supplemented with protease inhibitors. Lysates were incubated with antibody against HDAC4. After incubation with protein A beads (GE Healthcare, Little Chalfont, UK), washes were performed with lysis buffer. For the deacetylase assay, beads were resuspended in the assay buffer (50 mM TrisCl, pH 8; 137 mM NaCl; 2.7 mM KCl; and 1 mM $MgCl_2$) and incubated with Fluor-de-Lys Green Substrate (Enzo Life Sciences, Farmingdale, NY, USA), which comprises an acetylated lysine side chain, for 30 min at 37°C. Deacetylation of the substrate sensitizes it so that treatment with the developer produces a fluorophore. When added to the assay buffer, TSA was at 40 μM final concentration. For immunofluorescence, cells were fixed in 3% paraformaldehyde and permeabilized with 0.1% Triton-X100 in PBS. Next, coverslips were incubated with primary antibodies anti-HDAC4, anti-HMGB1 (Abcam), anti-SMAC (6, 19), and anti-DRP-1 (BD Biosciences). Finally, they were washed twice with PBS and incubated with 488-Alexa or 546-Alexa conjugated secondary antibodies (Invitrogen) and TRITC-phalloidin (Sigma-Aldrich). Cells were examined with a Leica SP confocal microscope.

RNA extraction, retrotranscription reaction, and quantitative PCR

Cells were harvested, and RNA was obtained using TRIzol reagent (Life Technologies, Gaithersburg, MD, USA). MMLV reverse transcriptase (Life Technologies) was used for retrotranscription, utilizing 1 μg of total RNA for reaction. qRT-PCR was performed using CFX96 (Bio-Rad, Hercules, CA, USA) and SYBR green technology (Kapa Biosystems, Woburn, MA, USA). Data were analyzed with the $\Delta\Delta C_t$ method, using the geometric mean of *HPRT* and β-*actin* for normalization. Data, from ≥3 independent experiments, were expressed as means ± SE and analyzed with Student's *t* test. qRT-PCR data with the inhibitor were obtained using the geometric mean of *HPRT*, β-*actin*, and *GAPDH* for normalization. All reactions were done in triplicate.

Cell cycle analysis

DNA staining was performed as described previously (6). For S-phase analysis, cells were grown for 3 h with 100 μM bromodeoxyuridine (BrdU). After fixation, coverslips were treated with 1 N HCl (10 min, in ice), followed by 20 min with 2 N HCl at room temperature. Mouse anti-BrdU (Sigma-Aldrich) was used as primary antibody. Nuclei were stained with Hoechst 33258 (Sigma-Aldrich).

Genomic DNA isolation and DNA sequencing

Genomic DNA was isolated and purified using the Qiagen kit (Qiagen, Valencia, CA, USA). PCRs were made using primers covering the different exons. All PCR products were sequenced with the Big Dye Terminator Sequencing RR-100 kit on the ABI PRISM 310 Genetic Analyzer platform (Applied Biosystems, Foster City, CA, USA) on both strands.

Chromatography

Cells were resuspended in the lysis buffer (50 mM TrisHCl, pH7.5; EDTA 0.5 mM; 120 mM NaCl; and Nonidet P-40 0,5%). After centrifugation at 12,000 rpm for 10 min, the extracts were loaded on a column packed with Superose 6 (GE Healthcare). As running buffer, 50 mM TrisHCl (pH 7.5), EDTA 0.5 mM, 120 mM NaCl, and Nonidet P-40 0.1% was used.

Gene set enrichment analysis (GSEA)

Analyses were performed using the GSEA software (http://www.broadinstitute.org/gsea/index.jsp). The list of putative MEF2 target genes was obtained from the Molecular Signature Database (http://www.broadinstitute.org/gsea/msigdb/index.jsp). At least 1000 permutations were performed using the "genes_set" permutation type for data obtained from cell lines or "phenotype " permutation type for data obtained for human tumors. Datasets for human tumors were taken from the U.S. National Center for Biotechnology Gene Expression Omnibus (GEO) database (http://www.ncbi.nlm.nih.gov/geo/). For cell lines, datasets of Mori GSE15026 (20) and Varma GSE32474 (21) were used. For human tumor samples, datasets of Desmedt GSE7390 (22) and Pawitan GSE1456 (23) were employed.

TCGA Kaplan-Meier analysis

Class IIa HDAC expression data were retrieved from the cBio Cancer Genomics Portal (http://www.cbioportal.org/public-portal/). Patients were subdivided into 2 groups: the first consisted of patients with increased expression of at least one member of the family (Z score >2), and with the remnant members having a Z score between -2 and $+2$. In patients that composed the second group, all class IIa HDAC members showed a Z score between -2 and $+2$. All ER^+ tumor samples were taken from the PAM50 Luminal gene expression signatures.

RESULTS

Expression levels of the different components of the MEF2/HDAC axis in breast cancer cell lines

To comprehend the role of the MEF2-HDAC axis in breast cancer, we investigated the expression of the different components of the axis, in breast cancer cell lines and in the nontransformed mammary epithelial cell line, MCF-10A (**Fig. 1*A–C***). The selected cell lines recapitulate genetic alterations commonly observed in breast cancer (Supplemental Table S1). Class IIa HDACs are heterogeneously expressed, and an association between class IIa levels and a breast cancer cell type cannot be evoked. HDAC5 and HDAC9 show the highest expression in luminal cell line T47D. By contrast, HDAC4 levels are elevated in the basal MDA-MB series. Also, HDAC7 is highly expressed in the triple-negative cells, with a peak in the *BRCA1*-mutated HCC1937 cells, where HDAC4 is almost undetectable (Fig. 1*A–C*). MEF2 transcription factors present a more homogenous pattern of expression. MEF2C is expressed at similar levels in all tested breast cancer cell lines, whereas MEF2A and MEF2D expression show some complementarity, well evident in SK-BR-3 and MCF-10A cells.

Immunofluorescence analysis was used to define the subcellular localization of HDAC4. We focused our attention on this deacetylase because it is highly expressed in several basal cell lines, and mutations have been reported in breast cancer (16). To evaluate HDAC4 nuclear-cytoplasmic shuttling, cells were also treated with leptomycin B, an inhibitor of nuclear export. HDAC4 positivity was validated by siRNA transfection (data not shown). In almost all cancer cell lines, HDAC4 shows a diffuse nuclear-cytoplasmic (pancellular) or cytoplasmic localization (Fig. 1*D*). Suppression of nuclear export rapidly promoted its nuclear accumulation, with the exception of MDA-MB-468 cells (Fig. 1*D*). Figure 1*E* exemplifies the analysis performed, showing the data for the luminal cell line MCF7 and the basal cell line MDA-MB-468. These results indicate that in all the tested cell lines, HDAC4 shuttles continuously between the nucleus and cytoplasm, and in MDA-MB-468 cells, there is a defect in its nuclear import.

To evaluate mutations of HDAC4 in the investigated breast cancer cell lines, we sequenced its coding region, from exon 2 to exon 27. Homozygous variations in the HDAC4 coding sequence were found in HCC1937, ZR-75-1, SK-BR-3 and the three MDA-MB cell lines (Supplemental Table S2). However, only in HCC1937 cells was a missense mutation (A786T in exon 18) found. To evaluate HDAC4 levels in breast tumors, immunohistochemistry analysis was performed on 21 cases (Supplemental Fig. S1 and Supplemental Table S3). We evaluated the intensity of HDAC4 staining and its subcellular localization. Similar to breast cancer cell lines, HDAC4 levels are highly variable among different breast tumors, without significant correlations with the proliferative rate or the ER and progesterone receptor (PR) status. Likewise, HDAC4 subcellular localization shows profound variations among the different samples but again without evident correlations with the clinical markers.

Class IIa HDACs-repressive influence on MEF2-dependent transcription in breast cancer cell lines

Because multiple alterations (nuclear-cytoplasmic shuttling, expression levels, point mutations) could potentially affect HDAC4 functions, a simple correlation between breast cancer aggressiveness and HDAC4 levels could be misleading. In principle, to be relevant, any alteration affecting HDAC4 in tumors should affect its repressive activity. According to this hypothesis, we decided to use HDAC4-repressive activity as a tool to unveil its correlation with breast cancer. Krüppel-like factor 2 (KLF2) is a well-known transcriptional target of the MEF2-HDAC axis (6, 24). We utilized KLF2 as a marker to estimate HDAC4-repressive influence. For these studies, we selected MCF7 and MDA-MB-231 cell lines as examples of luminal ER^+ and triple-negative cells.

To understand the role of HDAC4 in the regulation of KLF2 expression in breast cancer cells, MCF7 and MDA-MB-231 cells were silenced for HDAC4, and the mRNA level of the MEF2 target gene was measured by qRT-PCR. In both cell lines, KLF2 expression was not significantly affected by the down-regulation of HDAC4 (**Fig. 2*A***). The effectiveness of HDAC4 silencing was also verified by immunoblot (data not shown). Although HDAC4 is abundantly expressed in several breast cancer cell lines, other members of the family are expressed as well. These deacetylases could interact with MEF2s and overcome the down-regulation of HDAC4. Moreover, compensatory mechanisms have been reported when the expression of a single member of this family is silenced (25). Therefore, we investigated whether silencing of HDAC4 elicited the up-regulation of HDAC5, HDAC7 and HDAC9. As shown in Fig. 2*B*, in MCF7 cells, silencing of HDAC4 triggered the up-regulation of HDAC5, but not of HDAC7 and HDAC9. This response was not observed in MDA-MB-231 cells.

To investigate the role of class IIa HDACs, we decided to silence simultaneously at least 3 members. We focused our attention on HDAC4, HDAC5, and HDAC9,

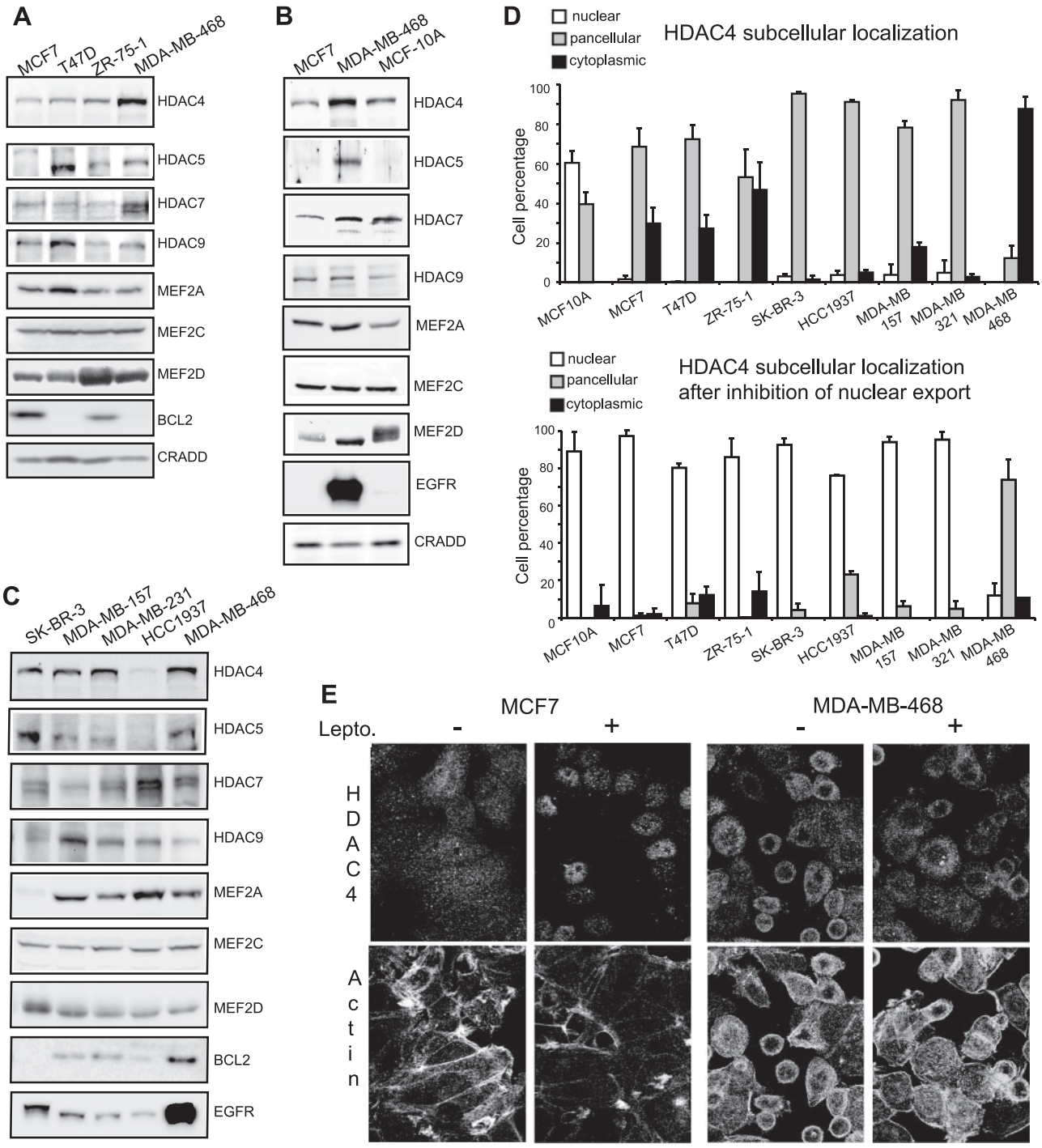

Figure 1. Analysis of HDAC class IIa expression in breast cancer cell lines. *A*) Cellular lysates of indicated breast cancer cell lines were subjected to immunoblot analysis using the specific antibodies. CRADD was used as loading control. *B*) Cellular lysates of indicated cell lines were subjected to immunoblot analysis using the specific antibodies. CRADD was used as loading control. *C*) Cellular lysates of the indicated breast cancer cell lines were subjected to immunoblot analysis using the specific antibodies. *D*) Quantitative analysis of HDAC4 subcellular localization in the indicated cell lines. Immunofluorescence analyses were performed as described in Materials and Methods to visualize HDAC4. When used, leptomycin B was added for 1 h. Approximately 300 cells, from 3 independent experiments, were scored. Data represent arithmetic means ± SD. *E*) Confocal pictures exemplifying the subcellular localization of HDAC4. Leptomycin B was added for 1 h as indicated. Immunofluorescence analysis was performed to visualize HDAC4 subcellular localization. TRITC-phalloidin was used to decorate actin filaments.

because they are phylogenetically closer. The effectiveness of the different siRNAs was also verified by immunoblot (data not shown). KLF2 mRNA was still unperturbed in MDA-MB-231 cells with down-regulated HDAC4, HDAC5, and HDAC9. By contrast, in MCF7 cells, the expression of the MEF2 target, KLF2, was

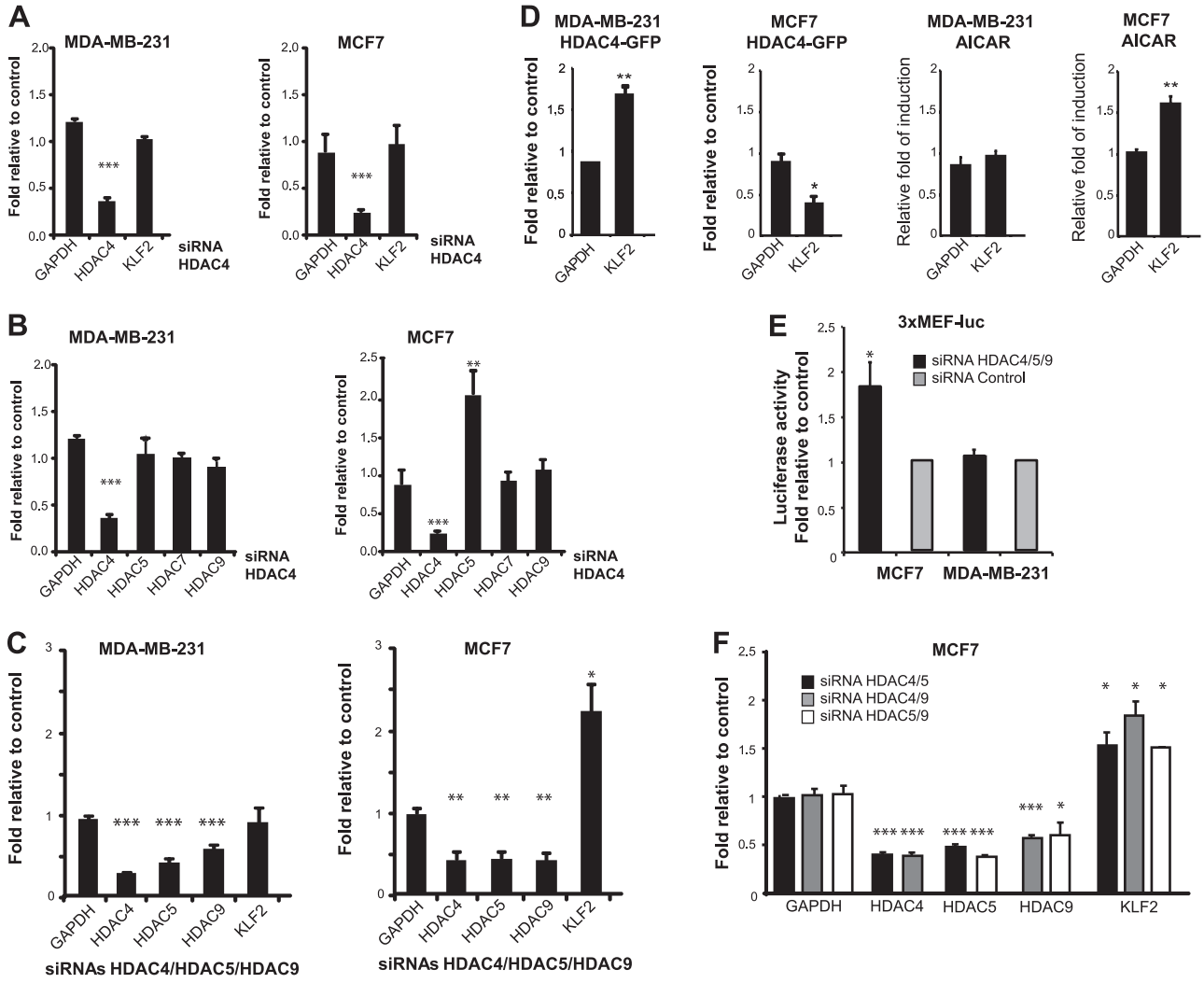

Figure 2. Regulation of KLF2 expression by class IIa HDACs in breast cancer cells. *A*) qRT-PCR analysis was performed to quantify mRNA levels of the MEF2 target gene *KLF2* and of *HDAC4* to verify silencing efficiency. *GAPDH* was used as control gene. MCF7 and MDA-MB-231 cells transfected with siRNA against HDAC4 were lysed, and mRNAs were extracted. Fold induction was calculated as the ratio relative to control siRNA-transfected cells. *B*) qRT-PCR analysis was performed to quantify mRNA levels of *HDAC4*, *HDAC5*, *HDAC7*, and *HDAC9*. *GAPDH* was used as control gene. MCF7 and MDA-MB-231 cells transfected with siRNA against HDAC4 were lysed, and mRNAs were extracted. Fold induction was calculated as the ratio relative to control siRNA-transfected cells. *C*) qRT-PCR analysis was performed to quantify mRNA levels of the MEF2 target gene *KLF2* and of *HDAC4*, *HDAC5*, and *HDAC9* to verify silencing efficiency. *GAPDH* was used as control gene. MDA-MB-231 and MCF7 cells cotransfected with siRNAs against HDAC4, HDAC5, and HDAC9 or with the same amount of a control siRNA were lysed, and mRNAs were extracted. Fold induction was calculated as the ratio relative to control siRNA-transfected cells. *D*) MCF7 and MDA-MB-231 cells expressing HDAC4-GFP or GFP were lysed, and mRNAs were extracted. qRT-PCR analysis was performed to quantify mRNA levels of *KLF2*. Fold induction was calculated as the ratio relative to GFP-tramsfected cells. MCF7 and MDA-MB-231 cells were treated with AICAR (200 μM) for 24 h. qRT-PCR analysis was performed to quantify mRNA levels of *KLF2*. *GAPDH* was used as control gene. Fold induction was calculated as the ratio relative to untreated cells. *E*) After 24 h from HDAC4, HDAC5, HDAC9, and control silencing, cells were transfected with 3xMEF2-Luc reporter (1 μg) and the internal control luciferase reporter pRL-CMV (20 ng) to normalize the transfection efficiency. Assays were performed 24 h later. *F*) qRT-PCR analysis was performed to quantify mRNA levels of the MEF2 target gene *KLF2*. *GAPDH* was used as control gene. MCF7 cells cotransfected with the indicated combinations of siRNAs against HDAC4, HDAC5, and HDAC9 or with the same amount of a control siRNA were lysed, and mRNAs were extracted. Fold induction was calculated as the ratio relative to control siRNA-transfected cells. Data are from 3 independent experiments. $*P < 0.05$; $**P < 0.01$; $***P < 0.005$.

up-regulated (Fig. 2*C*). To verify this result, we generated MCF7 and MDA-MB-231 cells stably expressing HDAC4-GFP or GFP alone. qRT-PCR analysis confirmed that in MCF7 cells, KLF2 is regulated by HDAC4. Surprisingly, KLF2 expression was up-regulated in MDA-MB-231 cells expressing HDAC4-GFP (Fig. 2*D*). However, it should be taken into account that retroviral infection with HDAC4-GFP elicited a strong inhibition of cell growth, as previously observed (26), which results in the selection of few clones positive for HDAC4. Hence, we used an alternative strategy to corroborate the differential requirement of class IIa HDACs, in the two cell lines. To release class IIa HDACs-mediated repression, we

promoted their export through the engagement of the AMP-activated protein kinase (AMPK; ref. 25). MDA-MB-231 and MCF7 cells were treated with the AMPK activator AICAR, and mRNA was isolated for qRT-PCR analysis. KLF2 levels were up-regulated after AICAR treatment only in MCF7 cells. Finally, transcription from a MEF2 artificial promoter was selectively augmented in MCF7 cells silenced for the different HDACs (Fig. 2*E*).

To elucidate which deacetylases are implicated in the repression of KLF2 expression in MCF7 cells, we evaluated the combination of two different siRNAs. As illustrated in Fig. 2*F*, silencing of two HDACs at a time was sufficient to up-regulate KLF2 levels, although less potently compared to the triple siRNA. Individual silencing of HDAC5 or HDAC9 was not sufficient to augment KLF2 mRNA (data not shown). We also reduced repressive influence of the HDAC4 multiprotein complex, and a different transcriptional regulation limited the effeact of class IIa HDACs on KLF2 expression in MDA-MB-231 cells. Class IIa HDACs seem to be dispensable for the control of KLF2 transcription in MDA-MB-231 cells. Hence, in the triple-negative cell line, the MEF2-HDAC axis could be altered. To answer this question, we initially compared the capability of class IIa HDACs to form a complex with MEF2s. Coimmunoprecipitation showed that in both cell lines, HDAC4 can be isolated in a complex with MEF2D (**Fig. 3*A***).

HDAC4 represses transcription by bridging the enzymatically active SMRT/N-CoR-HDAC3 complex to target promoters (27). After fractionation of cellular extracts overexpressing HDAC4 on a superose 6 column, enzymatic activity was found in a high-molecular-weight (HMW) complex with mass > 0.66 MDa (27). Hence, we investigated whether endogenous HDAC4 also could be isolated in an HMW complex and whether differences could be appreciated between the two cell lines. Immunoblotting of the different fractions visualized for HDAC4, MEF2D and HDAC3 are shown in Fig. 3*B*. Overall, the pattern is similar in the two cell lines. Only limited amounts of HDAC4 and MEF2D were visualized in fractions of >0.66 MDa. By contrast, HDAC3 was almost entirely found in fractions > 0.66 MDa.

To confirm that MEF2D and HDAC4 can interact in an HMW complex, the different fractions were immunoprecipitated for HDAC4 and visualized for MEF2D. We performed this experiment in MDA-MD-231 cells that express higher amounts of HDAC4. An enrichment of MEF2D in the >0.66-MDa complex and a reduction in the low-molecular-weight fractions can be appreciated in Fig. 3*B*. In summary, these studies indicate that in both cell lines, HDAC4 binds MEF2D and can form protein complexes of mass > 0.66 MDa. Theoretically, in both cell lines, HDAC4 should be competent for suppressing MEF2-dependent transcription.

To prove this assumption, we analyzed the deacetylase activity associated with HDAC4. Protein complexes containing HDAC4 were isolated using anti-HDAC4 antibody, and deacetylase activity was scored using an acetyl lysine as substrate. The deacetylase activity associated with HDAC4 was higher in MCF7 compared to MDA-MB-231 cells (Fig. 3*C*). This difference was even more impressive considering that much more HDAC4 was immunoprecipitated from MDA-MB-231 cells (Fig. 3*D*). Normalization of the enzymatic activity, relative to the amount of immunoprecipitated HDAC4, evidenced a 5-fold increase of HDAC4-associated deacetylase activity in MCF7 cells (Fig. 3*E*). Since HDAC3 provides an important contribution to the HDAC4-associated deacetylase activity, we analyzed HDAC3 levels in the two cell lines. HDAC3 levels were reduced in MDA-MB-231 compared to MCF7 cells (Fig. 3*F*).

Taking into account that KLF2 is a target of the MEF2-HDAC axis in breast cancer cells and that class IIa HDAC-repressive influence is reduced in MDA-MB-231 cells, its expression should be elevated in MDA-MB-231 compared to MCF7 cells. qRT-PCR analysis verified that KLF2 expression is almost 6-fold higher in MDA-MD-231 cells (Fig. 3*G*). We also evaluated whether KLF2 is subjected to different regulation in the two cell lines. The PI3K/AKT pathway can regulate KLF2 expression (28). Inhibition of this pathway has different consequences on KLF2 in the two cell lines (Fig. 3*H*). In MCF7 cells, the PI3K inhibitor LY294002 augmented KLF2 levels, whereas in MDA-MB-231 cells, it reduced KLF2 expression. This result indicates that KLF2 expression is under different regulation in the two cell lines.

Class IIa HDACs regulate survival of MCF7 cells

Having proved a repressive influence of class IIa HDACs in MCF7 cells, we decided to explore the contribution of these HDACs to cell proliferation. The simultaneous down-regulation of HDAC4/5/9 significantly affected proliferation in MCF7 but not in MDA-MB-231 cells (**Fig. 4*A***). Conversely, single silencing of HDAC4 was insufficient to reduce proliferation (Supplemental Fig. S2). Cytofluorimetric analysis did not revealed overt changes in cell-cycle profiles of MCF7 cells silenced for HDAC4, HDAC5, and HDAC9 (Fig. 4*B*). Paradoxically, a small rise in cells replicating the DNA was observed after BrdU staining (Fig. 4*C*). Next we evaluated whether class IIa HDACs could restrain apoptosis in MCF7 cells. Trypan blue assay revealed an increase in cell death when HDAC4, HDAC5, and HDAC9 levels were reduced after siRNA transfection (Fig. 4*D*). Apoptosis was confirmed by scoring the release of SMAC from mitochondria, a mitochondrial outer membrane permeabilization marker, and the accumulation of HMGB1 in the cytoplasm (Fig. 4*E*). In both assays, down-regulation of class IIa HDACs significantly increased the percentage of cells showing apoptotic features (Fig. 4*F*).

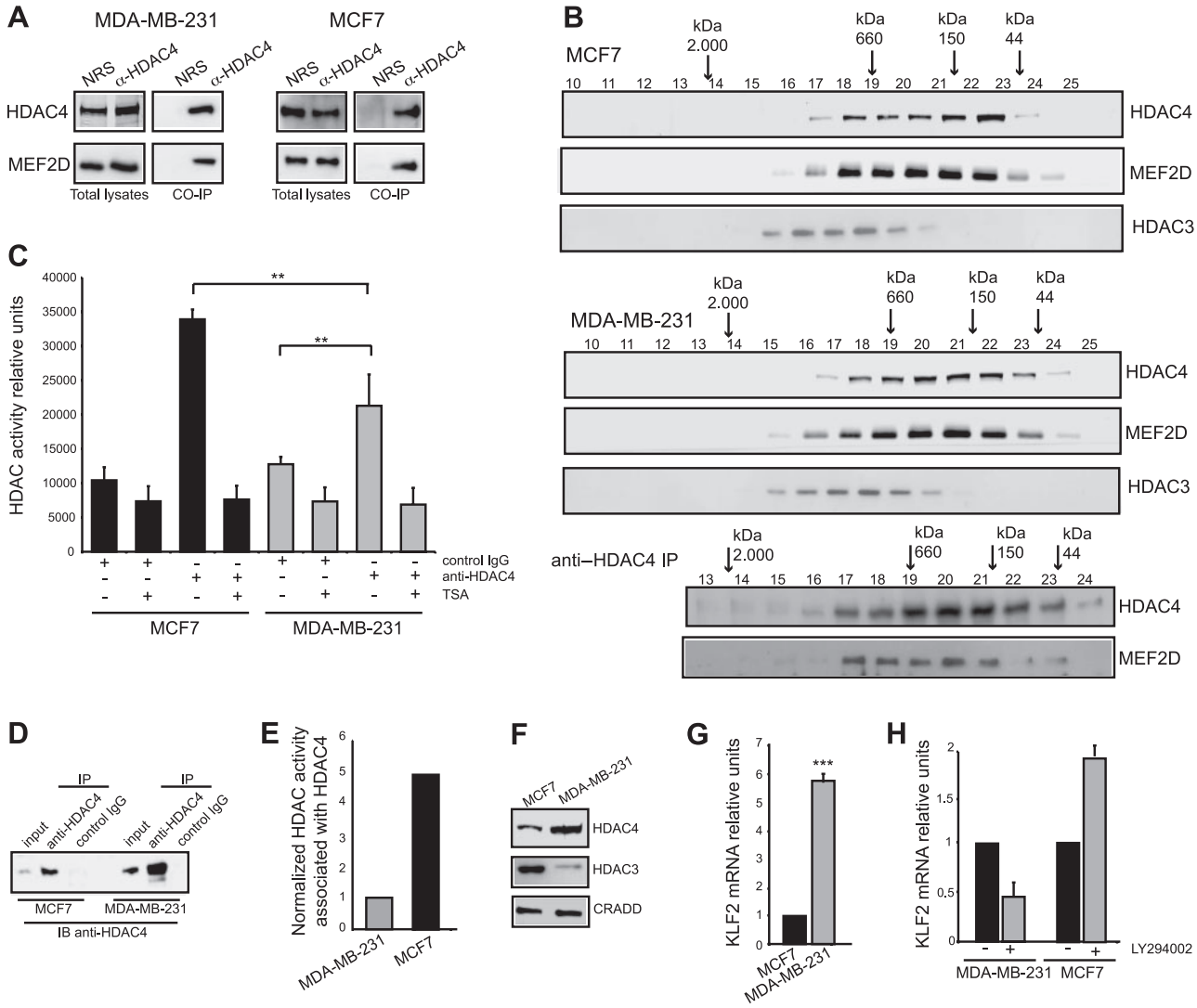

Figure 3. Understanding the differential contribution of class IIa HDACs in ER$^+$ (MCF7) and ER$^-$ (MDA-MB-231) breast cancer cells. *A*) Cellular lysates from MDA-MB-231 and MCF7 cells were immunoprecipitated using an anti-HDAC4 antibody or normal rabbit serum (NRS). Immunocomplexes were next probed with anti-MEF2D or anti-HDAC4 antibodies, as indicated. A fraction of the lysates before immunoprecipitation was used as input (total lysates). *B*) Cellular lysates from MDA-MB-231 and MCF7 cells were separated on a Superose 6 gel-filtration column. Fractions were analyzed for the presence of HDAC4, MEF2D, and HDAC3 by immunoblotting. Next, fractions from MDA-MB-231 cells were immunoprecipitated using the anti-HDAC4 antibody, and immunoblotting was performed with the anti-MEF2D or anti-HDAC4 antibodies. Arrows indicate the elution positions of molecular mas standards. *C*) Cellular lysates from MDA-MB-231 and MCF7 cells were immunoprecipitated using an anti-HDAC4 antibody or control rabbit immunoglobulin (IgG). After several washes, immunocomplexes were incubated with the Fluor de Lys substrate. TSA was used at 40 μM final concentration. Data are from 3 independent experiments. *D*) A fraction of the immunoprecipitations analyzed for the deacetylase activity was separated by SDS-PAGE, and after immunoblotting, HDAC4 was visualized using anti-HDAC4 antibody. *E*) Densitometric analysis was performed on the immunoblot in panel *B* to normalize HDAC activity to the amount of HDAC4 purified from the two cell lines. *F*) Cellular lysates generated from MCF7 and MDA-MB-231 cell lines were subjected to immunoblot analysis using specific antibodies as indicated. CRADD was used as loading control. *G*) qRT-PCR analysis was performed to compare KLF2 mRNA levels between MCF7 and MDA-MB-231 cells. Samples were normalized to *HPRT*, *GAPDH*, and β-*actin*. Fold induction was calculated as the ratio relative to KLF2 mRNA levels in MCF7 cells. Data are from ≥3 independent experiments. *H*) qRT-PCR analysis of KLF2 mRNA levels in MCF7 and MDA-MB-231 cells after treatment for 12 h with LY294002 (5 μM). Data are from ≥3 independent experiments. $*P < 0.05$; $**P < 0.01$; $***P < 0.005$.

Class IIa HDACs repress the expression of the proapoptotic gene Nur77/NR4A1 in MCF7 cells

Ectopic expression of KLF2 could not trigger apoptosis in MCF7 cells (data not shown). The nuclear orphan receptor Nur77/NR4A1 is another transcriptional target of the MEF2-HDAC complex, and it can elicit apoptosis (29). To gain insight on the prosurvival activity of class IIa HDACs, we analyzed whether the expression of Nur77 family members (Nur77/NR4A1, Nurr1/NR4A2, and NOR1/NR4A3) is repressed by these deacetylases in MCF7 cells. Only the expression of Nur77/NR4A1 was significantly up-regulated when class IIa HDACs were silenced (**Fig. 5*A***).

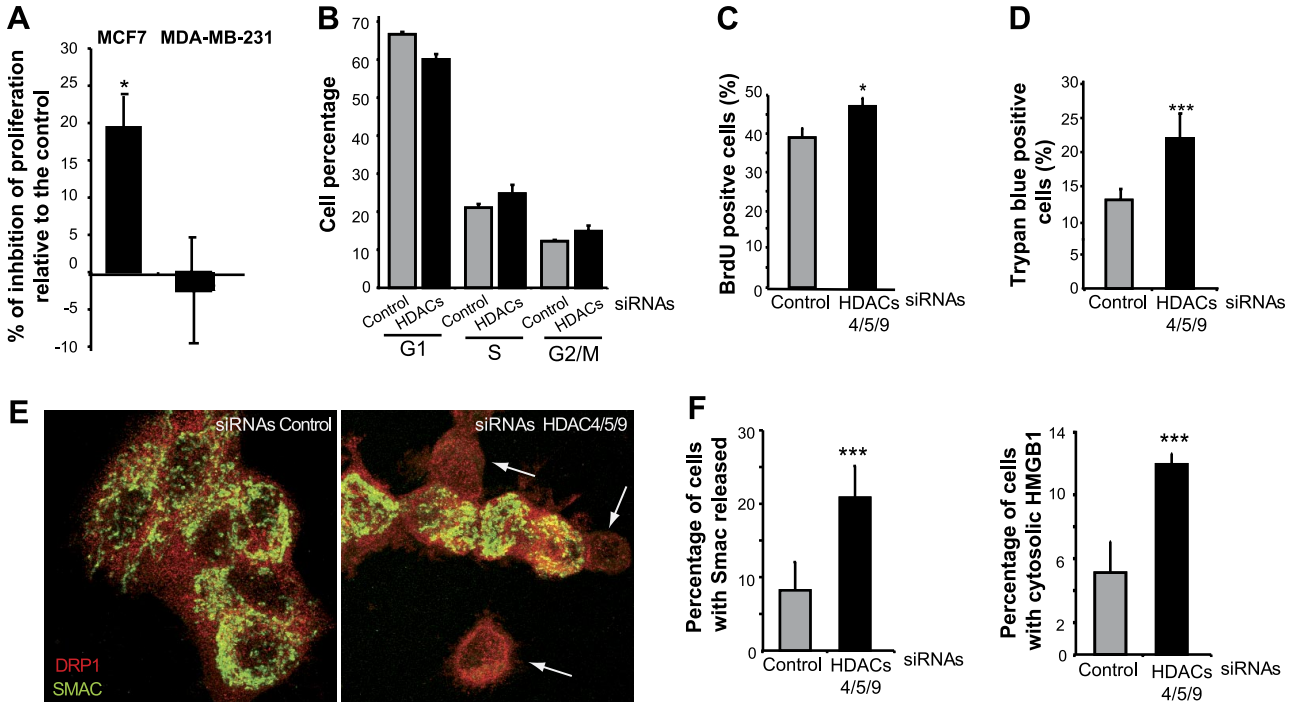

Figure 4. Class IIa HDACs control MCF7 cell survival. *A*) MCF7 and MDA-MB-231 cells were transfected with siRNAs against HDAC4, HDAC5, and HDAC9 or with the control siRNA. After 48 h, cells were counted. Data are presented as percentage of inhibition of the triple siRNAs relative to control and are expressed as means ± SD. $*P < 0.05$. *B*) MCF7 cells were transfected with siRNAs against HDAC4, HDAC5, and HDAC9 or with the control siRNA. After 48 h, cells were fixed, and cell cycle profiles were assessed by FACS analysis (means±SD, $n=3$). *C*) MCF7 cells were transfected with siRNAs against HDAC4, HDAC5, and HDAC9 or with the control siRNA. After 33 h, BrdU was added for 3 h, and then cells were processed for immunofluorescence (means±SD, $n=3$). *D*) MCF7 cells were transfected with siRNAs against HDAC4, HDAC5, and HDAC9 or with the control siRNA. After 48 h, cell death was analyzed after Trypan blue staining (means±SD, $n=3$). *E*) Confocal images illustrating the subcellular localization of SMAC and HMGB1 in MCF7 cells transfected with siRNAs against HDAC4, HDAC5, and HDAC9 or with the control siRNA. At 36 h after transfection, cells were fixed and processed for immunofluorescence. TRITC-phalloidin was used to decorate actin filaments and anti-DRP1 antibodies to stain the cytoplasm. Images are shown in pseudocolors. Arrows point to cells with released SMAC or HMGB1. *F*) Quantitative analysis of SMAC and HMGB1 localization as described in panel *E*.

In other cell lineages, HDAC7 plays an important role in the regulation of Nur77/NR4A1 expression. In MCF7 cells, silencing of HDAC7 influenced Nur77 expression only in combination with the silencing of other class IIa HDACs (unpublished results). These results imply that in breast cancer cells, HDAC7 affects Nur77 expression comparably to the other members of the family.

Next, we compared the expression levels of Nur77 family members between MCF7 and MDA-MB-231 cells. Contrary to KLF2, Nur77 levels were dramatically reduced in MDA-MB-231 cells; whereas expression of Nurr1 and NOR1 was equivalent in the two cell lines (Fig. 5*B*). Similar to KLF2, in MDA-MB-231 cells, the expression of Nur77 family members was unaffected by the triple silencing (Fig. 5*C*). Finally, we verified whether enhancing Nur77 levels in MCF7 cells could elicit apoptosis. Nur77s fused to GFP or GFP alone were transiently transfected in MCF7 cells, and apoptosis was evaluated by scoring the release of SMAC from mitochondria. As exemplified by representative immunofluorescence images (Fig. 5*D*) and by quantitative analysis (Fig. 5*E*), expression of Nur77 promoted SMAC release from mitochondria. The increase in apoptosis was confirmed by the elevated rate of procaspase-3 processing in Nur77-overexpressing cells (Fig. 5*F*).

Repression of the MEF2 signature correlates with aggressiveness of ER$^+$ tumors

Our study in breast cancer cell lines suggests that class IIa HDACs could influence MEF2-dependent transcription in ER$^+$ but not in ER$^-$ tumors. To explore this hypothesis, we compared the MEF2-trancriptional signature in different breast tumors. For this aim, we employed a list of genes that carry in their proximal promoter the MEF2-binding site (http://www.broadinstitute.org/gsea/msigdb/index.jsp). We de-

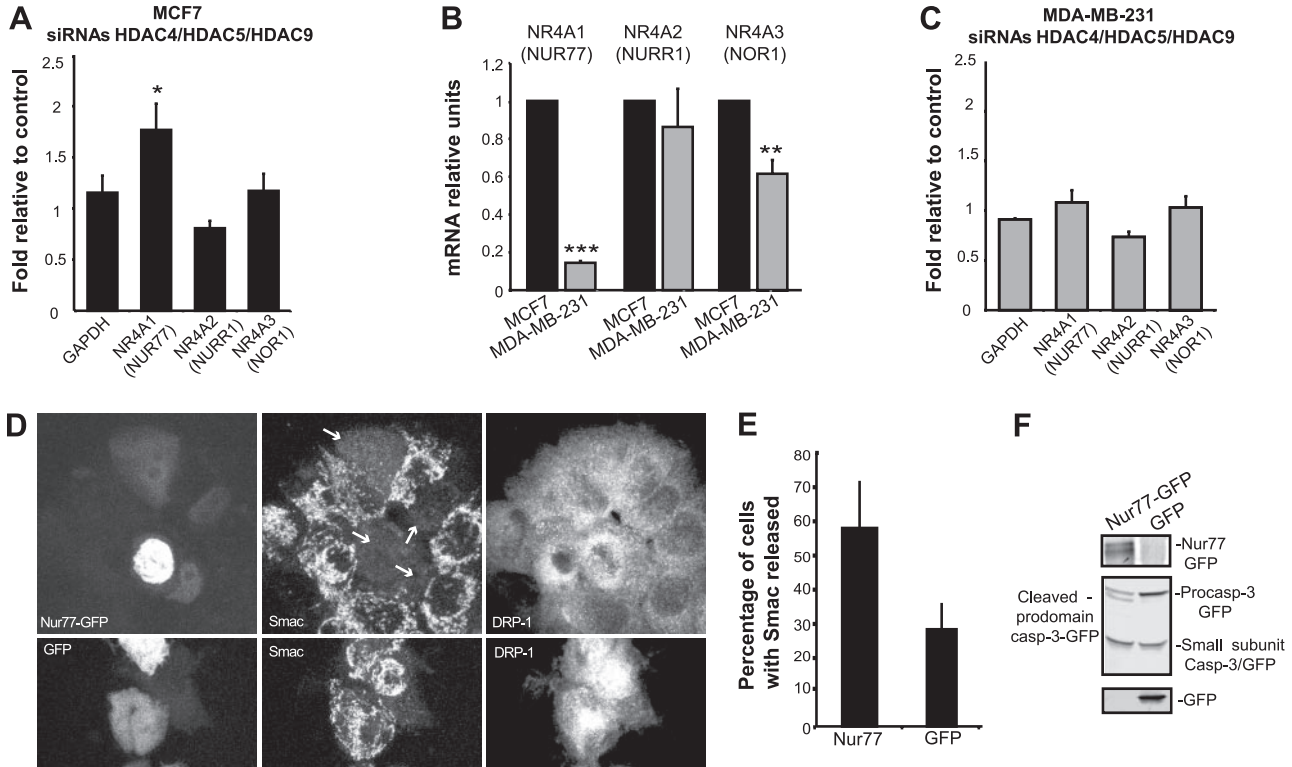

Figure 5. Class IIa HDACs repress NR4A1/NuR77 expression in MCF7 cells. *A*) qRT-PCR analysis was performed to quantify mRNA levels of the Nur77 family members *NR4A1*, *NR4A2*, and *NR4A3*. *GAPDH* was used as control gene. MCF7 cells cotransfected with siRNAs against HDAC4, HDAC5, and HDAC9 or with the same amount of a control siRNA were lysed, and mRNAs were extracted. Fold induction was calculated as the ratio relative to control siRNA-transfected cells. *B*) qRT-PCR analysis was performed to compare *NR4A1*, *NR4A2*, and *NR4A3* mRNA levels between MCF7 and MDA-MB-231 cells. Samples were normalized to *HPRT*, *GAPDH*, and β-*actin*. Fold induction was calculated as the ratio relative to *NR4A* mRNA levels in MCF7 cells. *C*) qRT-PCR analysis was performed to quantify mRNA levels of the Nur77 family members *NR4A1*, *NR4A2*, and *NR4A3*. *GAPDH* was used as control gene. MDA-MB-231 cells cotransfected with siRNAs against HDAC4, HDAC5, and HDAC9 or with a control siRNA were lysed, and mRNAs were extracted. Fold induction was calculated as the ratio relative to control siRNA-transfected cells. *D*) Confocal images illustrating the subcellular localization of SMAC in MCF7 cells transfected with NR4A1/Nur77-GFP or with GFP alone. At 24 h after transfection, cells were fixed and processed for immunofluorescence. Anti-DRP1 antibodies were used to stain the cytoplasm. Arrows point to cells with released SMAC. *E*) Quantitative analysis of SMAC localization as described in panel *D*. *F*) Caspase-3/GFP together with Nur77-GFP or GFP alone was transiently expressed in MCF7 cells. After 24 h, cell lysates were generated and subjected to immunoblotting using the anti-GFP antibody. $*P < 0.05$; $**P < 0.01$; $***P < 0.005$.

cided to exclude from the analysis MEF2 target genes that are modulated by ER (Supplemental Fig. S3). We began by comparing the expression levels of the MEF2 target genes in MCF7 and MDA-MB-231 cells, using GSEA and two different data sets (20, 21). **Figure 6*A*** illustrates a reduction in the expression of the MEF2 target genes in MCF7 cells compared to MDA-MB-231 cells ($P<0.001$ and $P<0.04$), which reflects the behavior of KLF2.

Next, we proved whether this correlation is also maintained in human breast cancers. We initially employed two different data sets comparing poorly differentiated tumors, classified grade 3 (G3) by histological grade, subdivided into ER^+ and ER^-. Figure 6*B* highlights that, similar to MCF7 and MDA-MB-231 cells, a negative correlation appears between G3 ER^+ tumors and the MEF2 signature with respect to ER^- G3 tumors ($P<0.025$ and $P<0.045$), using two different datasets (22, 23).

The down-regulation of the MEF2 signature in G3 ER^+ tumors prompted us to investigate the correlation between the signature and the aggressiveness of ER^+ tumors. When we compared the MEF2-signature in G1 and G2 *vs.* G3 ER^+ breast cancers, a down-regulation was evident using two different datasets (refs. 22, 23 and Fig. 6*C*; $P<0.001$, $P<0.001$, and $P<0.02$). On the contrary, when the analysis was performed between G1 and G2 ER^+ tumors, a differential correlation was not proved (Fig. 6*D*). Similarly, repression of the MEF2 signature was not discerned when G2 and G3 ER^- tumors were compared (Fig. 6*D*).

Targeting class IIa HDACs in ER^+ breast tumors

To validate the MEF2 signature used in the GSEA, we investigated whether modulation of class IIa HDACs could influence the expression of these genes. For this study, we used *N*-lauroyl-(L)-phenylalanine, a recently

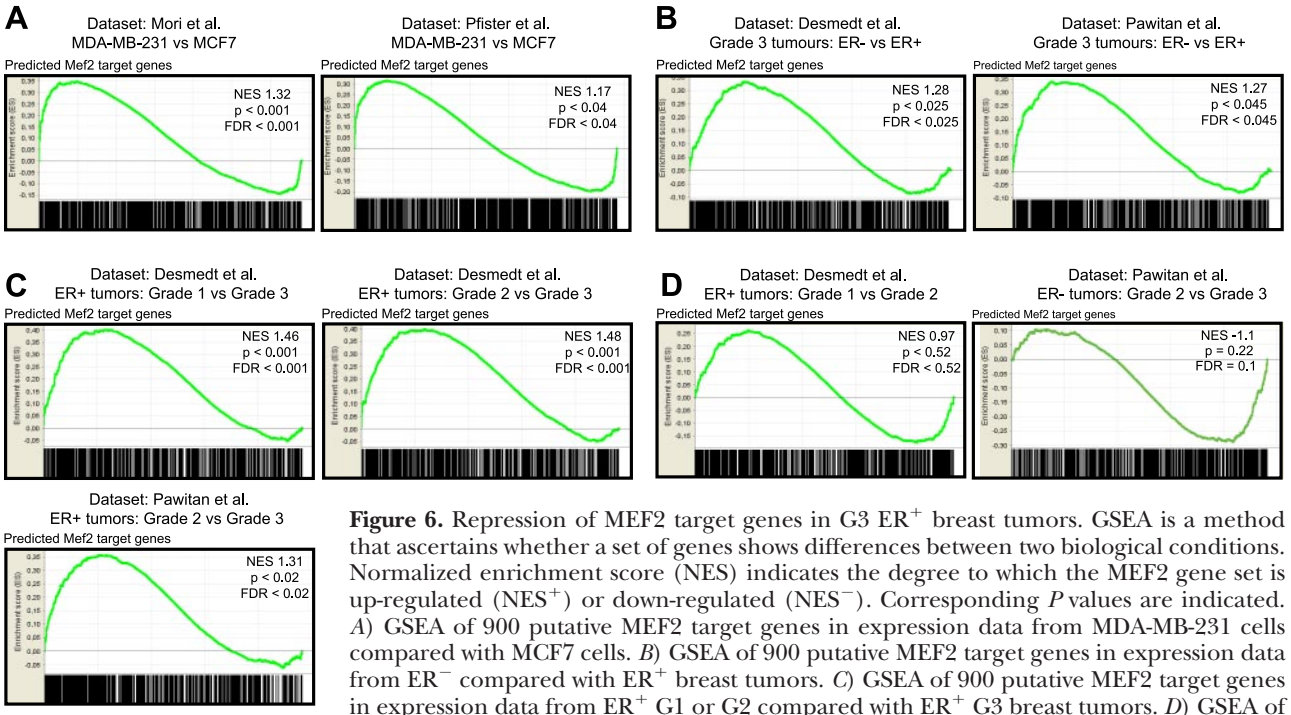

Figure 6. Repression of MEF2 target genes in G3 ER$^+$ breast tumors. GSEA is a method that ascertains whether a set of genes shows differences between two biological conditions. Normalized enrichment score (NES) indicates the degree to which the MEF2 gene set is up-regulated (NES$^+$) or down-regulated (NES$^-$). Corresponding *P* values are indicated. *A*) GSEA of 900 putative MEF2 target genes in expression data from MDA-MB-231 cells compared with MCF7 cells. *B*) GSEA of 900 putative MEF2 target genes in expression data from ER$^-$ compared with ER$^+$ breast tumors. *C*) GSEA of 900 putative MEF2 target genes in expression data from ER$^+$ G1 or G2 compared with ER$^+$ G3 breast tumors. *D*) GSEA of 900 putative MEF2 target genes in expression data from ER$^+$ G1 compared with ER$^+$ G2 or from ER$^-$ G2 compared with ER$^-$ G3 breast tumors.

identified class IIa specific histone deacetylase inhibitor (HDI; ref. 30). The deacetylase activity associated with immunoprecipitated HDAC4, but not with immunoprecipitated HDAC3, was inhibited by the HDI (Supplemental Fig. S4).

When MCF7 and MDA-MB-231 cells were treated with the HDI, proliferation impairment (IC_{50} at 48 h: 230±12 μM) and cell death were observed only MCF7 cells (**Fig. 7*A, B***). As for the siRNA experiments, growth of MDA-MB-231 cells was unaffected by the presence of the HDI. Next, we explored the effect of the class IIa HDI on a panel of MEF2 targets (NR4A1, KL2, KLF3, KLF5, MARK1, GADD45γ, IPO4, PPAP2A, and USP47), genes of the signature used in the GSEA. Figure 7*C* shows that expression of several MEF2 targets was significantly increased (>2-fold) in MCF7 cells treated with the HDI (KLF-2, NR4A1, KLF3, MARK1, and GADD45γ). This up-regulation was less evident in MDA-MB-231 cells. Here, only KLF3 induction mimicked the response observed in MCF7 cells. NR4A1 induction was less prominent, whereas KLF2, MARK1, and GADD45γ were not significantly up-regulated. By contrast, IPO4 induction was observed only in MDA-MB-231 cells. Of note, the HDI was a more potent inducer of the MEF2-dependent transcription with respect to the triple siRNA. The specificity of the antiproliferative effect elicited by the HDI was verified by comparing two compounds structurally resembling specific portions of the inhibitor: L-phenylalanine-methyl ester and dodecanoyl-(D/L)-homoserine. When dose-dependent studies were performed in MCF7 cells using the HDI and the two controls, effect on proliferation, induction of apoptosis, and activation of MEF2-dependent transcription were observed only in response to the class IIa inhibitor (Fig. 7*D–F*).

We also extended this study to other ER$^+$ and ER$^-$ cell lines (Supplemental Fig. S5). Overall, the ER$^-$ cells were resistant to the antiproliferative effect of the HDI and impotent in up-regulating Nur77 expression, whereas the ER$^+$ cell line (ZR-75-1) entered apoptosis and up-regulated Nur77 expression. These results prompted us to analyze the involvement of class IIa HDACs in the aggressiveness of ER$^+$ tumors. To begin to answer this question, we interrogated the Cancer Genome Atlas to find a correlation between survival and the expression levels of class IIa HDACs. The redundant role of class IIa HDACs inspired us to consider the different members of the family as a single entity. Patients with ER$^+$ tumors were subdivided into two groups: high and normal class IIa HDACs (see Materials and Methods). Kaplan-Meier analysis showed that patients with high class IIa HDAC expression had a median survival of 85 mo, compared to patients with low class IIa HDAC expression, who had a median survival of 114 mo (Fig. 7*G*).

DISCUSSION

Breast cancer is a heterogeneous disease in terms of morphological appearance, molecular features, behavior, and response to therapy (24). Our studies indicate that class IIa HDACs are heterogeneously expressed in different subtypes of breast cancer cell lines. This heterogeneity was also confirmed in breast tumors by exploring public-domain databases, such as GEO and

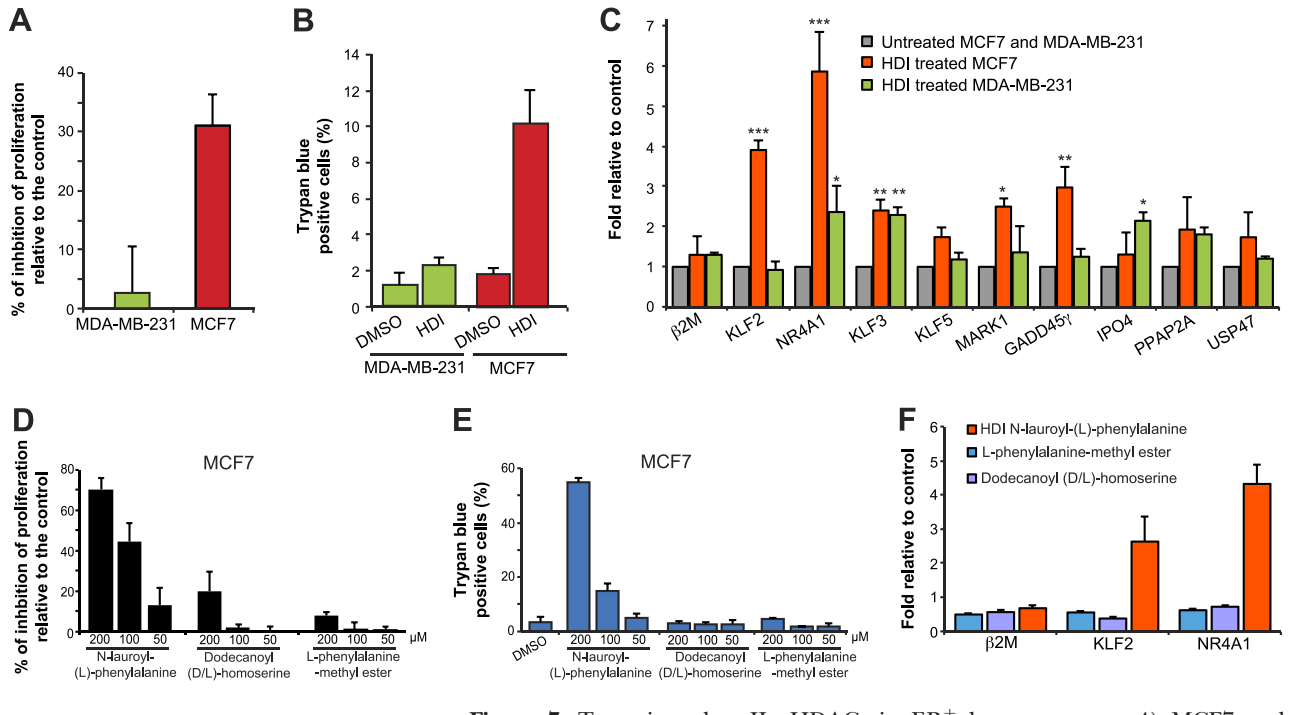

Figure 7. Targeting class IIa HDACs in ER$^+$ breast tumors. *A*) MCF7 and MDA-MB-231 cells were treated with 100 μM of the class IIa HDI *N*-lauroyl-(L)-phenylalanine. After 48 h, cells were counted. Data are presented as percentage of inhibition of the HDI relative to DMSO and are expressed as means ± SD. *B*) MCF7 and MDA-MB-231 cells were treated with HDI (100 μM). After 48 h, cell death was analyzed after Trypan blue staining (means±SD, n=3). *C*) qRT-PCR analysis was performed to evaluate the expression of a panel of MEF2 target genes selected from the set used in the GSEA. MCF7 and MDA-MB-231 cells were treated for 48 h with 100 μM HDI. Fold induction was calculated as the ratio relative to mRNA levels in untreated MCF7 and MDA-MB-231 cells, respectively. β2-Microglobulin was used as control. *D*) MCF7 cells were treated with the indicated concentrations of HDI and with two compounds, structurally resembling specific portions of the inhibitor: L-phenylalanine-methyl ester and dodecanoyl-(D/L)-homoserine. After 48 h, cells were counted. Data are presented as percentage of inhibition of the different compounds relative to DMSO and are expressed as means ± SD; n = 3. *E*) MCF7 cells were treated as in panel *D*. After 48 h, cell death was analyzed after Trypan blue staining (means±SD; n=3). *F*) qRT-PCR analysis was performed to evaluate the expression of the MEF2 target genes KLF2 and NR4A1. MCF7 cells were treated for 48 h with 100 μM of the indicated compounds. Fold induction was calculated as the ratio relative to mRNA levels in untreated MCF7 cells. β2-Microglobulin was used as control. *G*) Kaplan-Meier analysis based on class IIa HDACs expression using data from TCGA ER$^+$ breast cancers. All cases, n = 372; high class IIa HDAC expression cases, n = 29.

Oncomine, and by immunohistochemistry for HDAC4. A second feature of class IIa HDACs was redundancy. Class IIa HDACs act redundantly to suppress MEF2-dependent transcription, and compensatory circuits controlling their levels also exist (25). These characteristics hint that searching for a correlation between expression levels of a single member of the family and a particular breast cancer subtype could be an oversimplistic approach. Hence, we used a different strategy. We measured the contribution of class IIa HDACs to breast cancer indirectly, by ranking the expression levels of a list of putative MEF2 target genes. In this manner we have found a correlation between the down-regulation of several MEF2 targets and the aggressiveness of G3 ER$^+$ tumors. The association was further delineated by Kaplan-Meier analysis. High class IIa HDAC expression is associated with reduced survival in patients with ER$^+$ breast cancer.

Although ER positivity is generally considered a favorable prognostic marker, a substantial proportion of patients relapse despite endocrine therapy (31). The genomic grade index (GGI), a signature of 97 genes differentially expressed in breast cancers of low *vs.* high histological grade, has been proposed as a prognostic and predictive factor (32). Interestingly, patients with ER$^+$ tumors and high GGI had worse long-term recurrence-free survival (33). Many genes included in the GGI and also in different prognostic signatures are related to cell cycle and proliferation (34). Likewise, a protein signature of PI3K activation can predict the poor outcome of ER$^+$ breast cancer (35). Interestingly, the expression levels of the two MEF2 target genes KLF2 and NR4A1 inversely correlate with genes that mark cell proliferation in ER$^+$ tumors (Supplemental Table S4). Hence, it will be important to investigate whether connections between class IIa HDACs and

signaling pathways involved in the aggressiveness of ER^+ tumor exist.

How might repression of MEF2 target genes by class IIa HDACs enable more aggressive ER^+ breast cancer and lead to worse clinical outcomes? Experiments in MCF7 cells suggest that class IIa HDACs could affect cell survival. The prosurvival role of class IIa HDACs can be exemplified by the repressive influence on Nur77, a MEF2 target gene controlling apoptosis in certain conditions (29). Certainly, despite the finding, that Nur77 can assume apoptotic functions in MCF7, involvement of other MEF2 targets is highly predictable. Nur77/NR4A1 belongs to the family of orphan nuclear receptors (36). Nur77 can modulate apoptosis through both transcription-dependent and independent activities (37–39). Translocation of Nur77 into mitochondria can convert Bcl-2 into a proapoptotic factor (39), whereas in the nucleus, it can drive the expression of proapoptotic genes (37, 38). Interestingly, the prosurvival role of class IIa HDACs could have a therapeutic perspective. A class IIa HDAC inhibitor (30) elicited an antiproliferative response and apoptosis only in MCF7 and ZR-75-1 ER^+ cells. This response was coupled to the up-regulation of several MEF2 target genes, with Nur77 the more reactive.

In contrast to KLF2, expression of Nur77 was dramatically reduced in MDA-MB-231 cells. This result is not surprising, since MEF2 family members depend on the recruitment of, and cooperation with, other transcription factors to promote transcription of their target gene. In addition, MEF2 target genes (including KLF2 and Nurr77) can be regulated by factors alternative to MEF2, and MEF2 activity can be influenced by mechanisms in addition or alternative to class IIa HDAC binding (40). In fact, MDA-MB-231 cells are also less capable of augmenting Nur77 levels when class IIa HDACs are perturbed. These cells are largely emancipated from class IIa HDACs for the repression of this MEF2 target (41).

Unlike Nur77, in the triple-negative cells and in ER^- tumors, several MEF2 target genes are expressed at higher levels compared to ER^+ tumors. At the moment, the reason for this different behavior is unclear. In basal cancer cell lines, we observed that different alterations in class IIa HDACs could in principle promote the up-regulation of these target genes: point mutations (HCC1937), deficit in nuclear import (MDA-MB-468), reduced deacetylase activity associated with class IIa HDACs (MDA-MB-231). It is also possible that the activation of alterative signaling pathways renders superfluous the MEF2-HDAC axis. In summary, this first work on the MEF2-HDAC axis in breast cancer is clearly exploratory. Nonetheless, data presented here suggest a role of this axis in modulating outcomes in ER^+ breast cancer. FJ

This work was supported by Associazione Italiana Ricerca sul Cancro (AIRC; IG-10437). The authors thank Ivana Manini (Università di Udine), for help in the use of the cytofluorimeter, and Xiao-kun Zhang (Burnham Institute, San Diego, CA, USA), for providing Nur77 plasmid. A.C. received a Gemma del Cornò fellowship from AIRC.

REFERENCES

1. Yang, X. J., and Seto, E. (2008) The Rpd3/Hda1 family of lysine deacetylases: from bacteria and yeast to mice and men. *Nat. Rev. Mol. Cell Biol.* **9,** 206–218
2. Grozinger, C. M., and Schreiber, S. L. (2000) Regulation of histone deacetylase 4 and 5 and transcriptional activity by 14-3-3-dependent cellular localization. *Proc. Natl. Acad. Sci. U. S. A.* **97,** 7835–7840
3. McKinsey, T. A., Zhang, C. L., and Olson, E. N. (2001) Identification of a signal-responsive nuclear export sequence in class II histone deacetylases. *Mol. Cell. Biol.* **21,** 6312–6321
4. Paroni, G., Cernotta, N., Dello Russo, C., Gallinari, P., Pallaoro, M., Foti, C., Talamo, F., Orsatti, L., Steinkuhler, C., and Brancolini, C. (2008) PP2A regulates HDAC4 nuclear import. *Mol. Biol. Cell* **19,** 655–667
5. Kirsh, O., Seeler, J. S., Pichler, A., Gast, A., Muller, S., Miska, E., Mathieu, M., Harel-Bellan, A., Kouzarides, T., Melchior, F., and Dejean, A. (2002) The SUMO E3 ligase RanBP2 promotes modification of the HDAC4 deacetylase. *EMBO J.* **21,** 2682–2691
6. Cernotta, N., Clocchiatti, A., Florean, C., and Brancolini, C. (2011) Ubiquitin-dependent degradation of HDAC4, a new regulator of random cell motility. *Mol. Biol. Cell* **22,** 278–289
7. Haberland, M., Arnold, M. A., McAnally, J., Phan, D., Kim, Y., and Olson, E. N. (2007) Regulation of HDAC9 gene expression by MEF2 establishes a negative-feedback loop in the transcriptional circuitry of muscle differentiation. *Mol. Cell. Biol.* **27,** 518–525
8. Chen, J. F., Mandel, E. M., Thomson, J. M., Wu, Q., Callis, T. E., Hammond, S. M., Conlon, F. L., and Wang, D. Z. (2006) The role of microRNA-1 and microRNA-133 in skeletal muscle proliferation and differentiation. *Nat. Genet.* **38,** 228–233
9. Gregoire, S., and Yang, X. J. (2005) Association with class IIa histone deacetylases upregulates the sumoylation of MEF2 transcription factors. *Mol. Cell. Biol.* **25,** 2273–2287
10. Chang, S., McKinsey, T. A., Zhang, C. L., Richardson, J. A., Hill, J. A., and Olson, E. N. (2004) Histone deacetylases 5 and 9 govern responsiveness of the heart to a subset of stress signals and play redundant roles in heart development. *Mol. Cell. Biol.* **24,** 8467–8476
11. Cohen, T. J., Barrientos, T., Hartman, Z. C., Garvey, S. M., Cox, G. A., and Yao, T. P. (2009) The deacetylase HDAC4 controls myocyte enhancing factor-2-dependent structural gene expression in response to neural activity. *FASEB J.* **23,** 99–106
12. Milde, T., Oehme, I., Korshunov, A., Kopp-Schneider, A., Remke, M., Northcott, P., Deubzer, H. E., Lodrini, M., Taylor, M. D., von Deimling, A., Pfister, S., and Witt, O. (2010) HDAC5 and HDAC9 in medulloblastoma: novel markers for risk stratification and role in tumor cell growth. *Clin. Cancer Res.* **16,** 3240–3252
13. Rad, R., Rad, L., Wang, W., Cadinanos, J., Vassiliou, G., Rice, S., Campos, L. S., Yusa, K., Banerjee, R., Li, M. A., de la Rosa, J., Strong, A., Lu, D., Ellis, P., Conte, N., Yang, F. T., Liu, P., and Bradley, A. (2010) PiggyBac transposon mutagenesis: a tool for cancer gene discovery in mice. *Science* **330,** 1104–1107
14. Clocchiatti, A., Florean, C., and Brancolini, C. (2011) Class IIa HDACs: from important roles in differentiation to possible implications in tumourigenesis. *J. Cell. Mol. Med.* **15,** 1833–1846
15. Chin, K., DeVries, S., Fridlyand, J., Spellman, P. T., Roydasgupta, R., Kuo, W. L., Lapuk, A., Neve, R. M., Qian, Z., Ryder, T., Chen, F., Feiler, H., Tokuyasu, T., Kingsley, C., Dairkee, S., Meng, Z., Chew, K., Pinkel, D., Jain, A., Ljung, B. M., Esserman, L., Albertson, D. G., Waldman, F. M., and Gray, J. W. (2006) Genomic and transcriptional aberrations linked to breast cancer pathophysiologies. *Cancer Cell.* **10,** 529–541
16. Sjoblom, T., Jones, S., Wood, L. D., Parsons, D. W., Lin, J., Barber, T. D., Mandelker, D., Leary, R. J., Ptak, J., Silliman, N., Szabo, S., Buckhaults, P., Farrell, C., Meeh, P., Markowitz, S. D., Willis, J., Dawson, D., Willson, J. K., Gazdar, A. F., Hartigan, J., Wu, L., Liu, C., Parmigiani, G., Park, B. H., Bachman, K. E., Papadopoulos, N., Vogelstein, B., Kinzler, K. W., and Vel-

culescu, V. E. (2006) The consensus coding sequences of human breast and colorectal cancers. *Science* **314,** 268–274
17. Schuetz, C. S., Bonin, M., Clare, S. E., Nieselt, K., Sotlar, K., Walter, M., Fehm, T., Solomayer, E., Riess, O., Wallwiener, D., Kurek, R., and Neubauer, H. J. (2006) Progression-specific genes identified by expression profiling of matched ductal carcinomas in situ and invasive breast tumors, combining laser capture microdissection and oligonucleotide microarray analysis. *Cancer Res.* **66,** 5278–5286
18. Ozdag, H., Teschendorff, A. E., Ahmed, A. A., Hyland, S. J., Blenkiron, C., Bobrow, L., Veerakumarasivam, A., Burtt, G., Subkhankulova, T., Arends, M. J., Collins, V. P., Bowtell, D., Kouzarides, T., Brenton, J. D., and Caldas, C. (2006) Differential expression of selected histone modifier genes in human solid cancers. *BMC Genomics* **7,** 90
19. Henderson, C. J., Aleo, E., Fontanini, A., Maestro, R., Paroni, G., and Brancolini, C. (2005) Caspase activation and apoptosis in response to proteasome inhibitors. *Cell Death Differ.* **12,** 1240–1254
20. Mori, S., Chang, J. T., Andrechek, E. R., Matsumura, N., Baba, T., Yao, G., Kim, J. W., Gatza, M., Murphy, S., and Nevins, J. R. (2009) Anchorage-independent cell growth signature identifies tumors with metastatic potential. *Oncogene* **28,** 2796–2805
21. Pfister, T. D., Reinhold, W. C., Agama, K., Gupta, S., Khin, S. A., Kinders, R. J., Parchment, R. E., Tomaszewski, J. E., Doroshow, J. H., and Pommier, Y. (2009) Topoisomerase I levels in the NCI-60 cancer cell line panel determined by validated ELISA and microarray analysis and correlation with indenoisoquinoline sensitivity. *Mol. Cancer Ther.* **8,** 1878–1884
22. Desmedt, C., Piette, F., Loi, S., Wang, Y., Lallemand, F., Haibe-Kains, B., Viale, G., Delorenzi, M., Zhang, Y., d'Assignies, M. S., Bergh, J., Lidereau, R., Ellis, P., Harris, A. L., Klijn, J. G., Foekens, J. A., Cardoso, F., Piccart, M. J., Buyse, M., and Sotiriou, C. (2007) Strong time dependence of the 76-gene prognostic signature for node-negative breast cancer patients in the TRANSBIG multicenter independent validation series. *Clin. Cancer Res.* **13,** 3207–3214
23. Pawitan, Y., Bjohle, J., Amler, L., Borg, A. L., Egyhazi, S., Hall, P., Han, X., Holmberg, L., Huang, F., Klaar, S., Liu, E. T., Miller, L., Nordgren, H., Ploner, A., Sandelin, K., Shaw, P. M., Smeds, J., Skoog, L., Wedren, S., and Bergh, J. (2005) Gene expression profiling spares early breast cancer patients from adjuvant therapy: derived and validated in two population-based cohorts. *Breast Cancer Res.* **7,** R953–964
24. Kumar, A., Hoffman, T. A., Dericco, J., Naqvi, A., Jain, M. K., and Irani, K. (2009) Transcriptional repression of Kruppel like factor-2 by the adaptor protein p66shc. *FASEB J.* **23,** 4344–4352
25. Mihaylova, M. M., Vasquez, D. S., Ravnskjaer, K., Denechaud, P. D., Yu, R. T., Alvarez, J. G., Downes, M., Evans, R. M., Montminy, M., and Shaw, R. J. (2011) Class IIa histone deacetylases are hormone-activated regulators of FOXO and mammalian glucose homeostasis. *Cell* **145,** 607–621
26. Huang, Y., Tan, M., Gosink, M., Wang, K. K., and Sun, Y. (2002) Histone deacetylase 5 is not a p53 target gene, but its overexpression inhibits tumor cell growth and induces apoptosis. *Cancer Res.* **62,** 2913–2922
27. Fischle, W., Dequiedt, F., Hendzel, M. J., Guenther, M. G., Lazar, M. A., Voelter, W., and Verdin, E. (2002) Enzymatic activity associated with class II HDACs is dependent on a multiprotein complex containing HDAC3 and SMRT/N-CoR. *Mol. Cell* **9,** 45–57
28. Zhang, C., Elkahloun, A. G., Liao, H., Delaney, S., Saber, B., Morrow, B., Prendergast, G. C., Hollander, M. C., Gills, J. J., and Dennis, P. A. (2011) Expression signatures of the lipid-based Akt inhibitors phosphatidylinositol ether lipid analogues in NSCLC cells. *Mol. Cancer Ther.* **10,** 1137–1148
29. Dequiedt, F., Kasler, H., Fischle, W., Kiermer, V., Weinstein, M., Herndier, B. G., and Verdin, E. (2003) HDAC7, a thymus-specific class II histone deacetylase, regulates Nur77 transcription and TCR-mediated apoptosis. *Immunity* **18,** 687–698
30. Haus, P., Korbus, M., Schroder, M., and Meyer-Almes, F. J. (2011) Identification of selective class II histone deacetylase inhibitors using a novel dual-parameter binding assay based on fluorescence anisotropy and lifetime. *J. Biomol. Screen* **16,** 1206–1216
31. Musgrove, E. A., and Sutherland, R. L. (2009) Biological determinants of endocrine resistance in breast cancer. *Nat. Rev. Cancer* **9,** 631–643
32. Loi, S., Haibe-Kains, B., Desmedt, C., Lallemand, F., Tutt, A. M., Gillet, C., Ellis, P., Harris, A., Bergh, J., Foekens, J. A., Klijn, J. G., Larsimont, D., Buyse, M., Bontempi, G., Delorenzi, M., Piccart, M. J., and Sotiriou, C. (2007) Definition of clinically distinct molecular subtypes in estrogen receptor-positive breast carcinomas through genomic grade. *J. Clin. Oncol.* **25,** 1239–1246
33. Liedtke, C., Hatzis, C., Symmans, W. F., Desmedt, C., Haibe-Kains, B., Valero, V., Kuerer, H., Hortobagyi, G. N., Piccart-Gebhart, M., Sotiriou, C., and Pusztai, L. (2009) Genomic grade index is associated with response to chemotherapy in patients with breast cancer *J. Clin. Oncol.* **27,** 3185–3191
34. Sotiriou, C., and Piccart, M. J. (2007) Taking gene-expression profiling to the clinic: when will molecular signatures become relevant to patient care? *Nat. Rev. Cancer* **7,** 545–553
35. Miller, T. W., Hennessy, B. T., Gonzalez-Angulo, A. M., Fox, E. M., Mills, G. B., Chen, H., Higham, C., Garcia-Echeverria, C., Shyr, Y., and Arteaga, C. L. (2010) Hyperactivation of phosphatidylinositol-3 kinase promotes escape from hormone dependence in estrogen receptor-positive human breast cancer. *J. Clin. Invest.* **120,** 2406–2413
36. Moll, U. M., Marchenko, N., and Zhang, X. K. (2006) p53 and Nur77/TR3 - transcription factors that directly target mitochondria for cell death induction. *Oncogene* **25,** 4725–4743
37. Mullican, S. E., Zhang, S., Konopleva, M., Ruvolo, V., Andreeff, M., Milbrandt, J., and Conneely, O. M. (2007) Abrogation of nuclear receptors Nr4a3 and Nr4a1 leads to development of acute myeloid leukemia. *Nat. Med.* **13,** 730–735
38. Rajpal, A., Cho, Y. A., Yelent, B., Koza-Taylor, P. H., Li, D., Chen, E., Whang, M., Kang, C., Turi, T. G., and Winoto, A. (2003) Transcriptional activation of known and novel apoptotic pathways by Nur77 orphan steroid receptor. *EMBO J.* **22,** 6526–6536
39. Lin, B., Kolluri, S. K., Lin, F., Liu, W., Han, Y. H., Cao, X., Dawson, M. I., Reed, J. C., and Zhang, X. K. (2004) Conversion of Bcl-2 from protector to killer by interaction with nuclear orphan receptor Nur77/TR3. *Cell* **116,** 527–540
40. Potthoff, M. J., and Olson, E. N. (2007) MEF2: a central regulator of diverse developmental programs. *Development* **134,** 4131–4140
41. Chinnaiyan, P., Varambally, S., Tomlins, S. A., Ray, S., Huang, S., Chinnaiyan, A. M., and Harari, P. M. (2006) Enhancing the antitumor activity of ErbB blockade with histone deacetylase (HDAC) inhibition. *Int. J. Cancer* **118,** 1041–1050

Received for publication June 1, 2012.
Accepted for publication November 5, 2012.